Spectrochimica Acta Part A: Molecular and Biomolecular Spectroscopy 230 (2020) 118075

Contents lists available at ScienceDirect

Spectrochimica Acta Part A: Molecular and Biomolecular Spectroscopy

journal homepage: www.elsevier.com/locate/saa

Short Communication

A coumarin-fused '*off-on*' fluorescent probe for highly selective detection of hydrazine

Mei Wang [a], Xiaoli Wang [a], Xueyan Li [a,b], Ziqi Yang [a], Zhenbo Guo [a,b], Jiangyan Zhang [a,c], Jingjun Ma [d,**], Chao Wei [a,b,c,*]

[a] College of Chemistry and Environmental Science, Hebei University, Baoding 071002, China
[b] Key Laboratory of Chemical Biology of Hebei Province, Hebei University, Baoding 071002, China
[c] Key Laboratory of Medicinal Chemistry and Molecular Diagnosis of Ministry of Education, Hebei University, Baoding 071002, China
[d] College of Science and Technology, Hebei Agricultural University, Huanghua 061100, China

ARTICLE INFO

Article history:
Received 13 August 2019
Received in revised form 10 January 2020
Accepted 15 January 2020
Available online 16 January 2020

Keywords:
Hydrazine
Highly selective
Large *off-on* response
Fluorescent probe
Cellular imaging

ABSTRACT

Hydrazine is a kind of widely used industrial raw material and a toxic biochemical reagent. Due to its toxic to organisms, hydrazine has been classified to be a hazardous environmental pollutant. It is urgent to develop fluorescent probe tools for selective sensitivity detection of hydrazine in the environment and the body. We developed here a new coumarin-based fluorescent probe for hydrazine detection. The probe can selectively detect hydrazine over other environmental and endogenous interfering analytes with a large *off-on* fluorescence response. The detection limit is 8.55 ppb, which is well below the allowed threshold limit value. The sensing mechanism is hydrazine-induced pyrazole ring formation, which is confirmed by HRMS and DFT calculation methods. Additionally, the probe could also be applied for hydrazine imaging in living HeLa cells.

© 2020 Published by Elsevier B.V.

1. Introduction

Hydrazine, a colorless liquid inorganic compound, is highly reductive and basic, which is used as corrosion inhibitors in heating system [1]. As an important industrial raw material, hydrazine is widely applied to manufacture pharmaceuticals, pesticides, and chemical dyes, etc. Meanwhile, it is also used as a high-energy fuel for rocket-propulsion and missile systems. However, hydrazine is famous for its high toxicity, which can enter the body through breathing, osmosis, and other ways, and further damage the lungs, liver, kidneys and nervous system. It has been classified as a probable human carcinogen by the U.S. Environmental Protection Agency (EPA), and the minimum threshold limit value is set as 10 ppb [2]. Although hydrazine is not endogenously produced, some drugs can be metabolized to hydrazine in the human body and further endangers health. Therefore, the selective recognition and sensitive detection of trace hydrazine in environment and biological systems have been attracting increasing attention.

Conventional detection techniques for hydrazine mainly include titrimetry [3], electrochemical method [4–5], chromatography [6–7], and chemiluminescence [8]. However, comparing with traditional methods, fluorescence analysis has been widely applied for the detection of hydrazine because of its excellent selectivity, high sensitivity, especially non-invasive damage to biological samples [9–10]. To date, Based on its basicity and nucleophilicity, many sensing strategies for hydrazine have been found to design fluorescent probes, mainly including the hydrazinolysis of phenol acetate [11–19], the nucleophilic addition-intramolecular cyclization-elimination cascade reaction of keto ester [20–24] or halogen-ester [25–29], the Gabriel amine synthesis mechanism [30–34], hydrazone formation [35–45], pyrazole forming [46–50], and others [51–59]. High selectivity is the major challenge for hydrazine probes. However, the ester-based fluorescent probes might suffer from chemically unstable, and hydrazone formation-based probes might be interfered by other amines and hydrazine analogs. In contrast, the pyrazole forming and the Gabriel amine synthesis strategy would be the better choice for construction hydrazine fluorescent probe with high selectivity.

Herein, we reported a coumarin-fused hydrazine fluorescent probe **1** using the pyrazole forming strategy. Coumarin was used as fluorophore because of its high fluorescence quantum yield and excellent light stability. The ynone group in the 3-position of coumarin can not only quench fluorescence by photo-induced electron transfer (PET) effect but also serve as a reactive unit of hydrazine. The selectivity and sensitivity of the probe were examined in the PBS buffer solution, the sensing mechanism was confirmed by HRMS and DFT calculation

* Correspondence to: C. Wei, College of Chemistry and Environmental Science, Hebei University, Baoding 071002, China.
** Correspondence to: J. Ma, College of Science and Technology, Hebei Agricultural University, Huanghua 061100, China.
E-mail addresses: mjjwjpmartin@sina.com (J. Ma), weichao@hbu.edu.cn (C. Wei).

https://doi.org/10.1016/j.saa.2020.118075
1386-1425/© 2020 Published by Elsevier B.V.

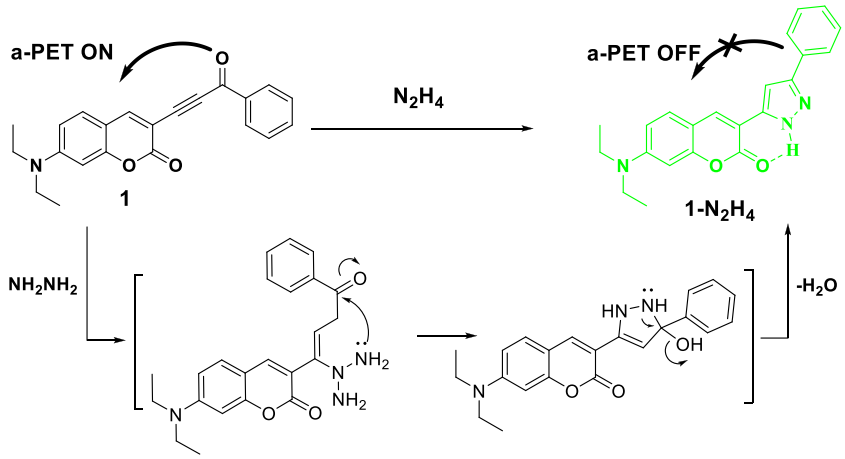

Scheme 1. The sensing mechanism of probe **1** with hydrazine.

methods, and the bioimaging of hydrazine in HeLa cells using probe **1** was finally evaluated.

2. Experimental section

2.1. Materials and instruments

All reagents including salicylaldehyde, trimethylsilylacetylene, $PdCl_2(PPh_3)_2$, CuI, and benzoyl bromide were purchased from *J&K* Scientific Co. Ltd. with the purity >95%. All the solvents were produced by professional suppliers. All reagents and solvents were used directly without further purification.

NMR spectra were recorded on Advance 600 MHz (Bruker). High-Resolution Mass Spectrometry (HRMS) spectra were determined using 7.0 T FTICR-MS (Varian). UV–vis spectra and fluorescence spectra were obtained using Cary 5000 Bio (Agilent) and F-7000 spectrophotometer (Hitachi), respectively. Bioimaging of cells was collected on a confocal microscope (Zeiss LSM 880).

The theoretical calculations were performed based on DFT (density functional theory) at the M062X/6-311d level in Gaussian 09 software. The solvent effect on molecular geometries was included by means of the polarizable continuum model (PCM).

2.2. Synthesis

2.2.1. Synthesis of 7-diethylamino-3-(trimethylsilyl)ethynylcoumarin (*3*)

Compound **2** (296 mg, 1.00 mmol) was dissolved in DMF (10 mL). $PdCl_2(PPh_3)_2$ (35 mg, 0.05 mmol, 5.0 mol%), CuI (9.5 mg, 0.05 mmol, 5.0 mol%), and (trimethylsilyl)acetylene (424 μL, 3.00 mmol) were added. The mixture was stirred at 60 °C for 5 h. After cooling to room temperature, the solution was diluted with CH_2Cl_2, washed with saturated NH_4Cl solutions, water and saturated NaCl solutions. The organic layer was dried, evaporated, and the residue was purified with column chromatography to give yellow solid (250 mg, yield: 80%). ^{1}H NMR (600 MHz, $CDCl_3$) δ 7.74 (s, 1H), 7.20 (d, J = 12.0 Hz, 1H), 6.55 (dd, J = 9.0, 2.4 Hz, 1H), 6.45 (d, J = 1.8 Hz, 1H), 3.41 (dd, J = 13.8, 6.6 Hz, 4H), 1.20 (t, J = 7.2 Hz, 6H), 0.25 (s, 9H).

2.2.2. Synthesis of 7-diethylamino-3-ethynylcoumarin (*4*)

Compound **3** (313 mg, 1.00 mmol) and K_2CO_3 (415 mg, 3.00 mmol) were dissolved in CH_3OH (15 mL). The mixture was stirred at room temperature overnight. After reaction completion, the mixture was diluted with CH_2Cl_2, washed with water and saturated NaCl solutions. The organic layer was dried, evaporated, and the residue was purified with column chromatography to give yellow solid (205 mg, yield: 85%). ^{1}H NMR (600 MHz, $CDCl_3$) δ 7.73 (s, 1H), 7.19 (d, J = 9.0 Hz, 1H), 6.55 (d, J = 8.4 Hz, 1H), 6.41 (s, 1H), 3.40 (dd, J = 14.4, 7.4 Hz, 4H), 3.22 (s, 1H), 1.19 (t, J = 7.2 Hz, 6H).

2.2.3. Synthesis of 7-diethylamino-3-(3-oxo-3-phenyl prop-1-yn-1-yl) coumarin (*1*)

Compound **4** (241 mg, 1.00 mmol), $PdCl_2(PPh_3)_2$ (35 mg, 0.05 mmol, 5.0 mol%), CuI (9.5 mg, 0.05 mmol, 5.0 mol%) and 1-bromo-4-nitrobenzene (222 mg, 1.20 mmol) were dissolved in anhydrous DMF (10 mL), and then anhydrous TEA (5 mL) was added to the system. The mixture was stirred at 80 °C for 5 h. After cooling to room temperature, the solution was diluted with CH_2Cl_2, washed with saturated NH_4Cl solutions, water, and saturated NaCl solutions. The organic layer was dried, evaporated, and the residue was purified with column chromatography to give a bright yellow solid (187 mg, yield: 54%). ^{1}H NMR (600 MHz, $CDCl_3$) δ 8.32 (d, J = 7.2 Hz, 2H), 7.97 (s, 1H), 7.60 (t, J = 7.2 Hz, 1H), 7.51 (t, J = 7.2 Hz, 2H), 7.27 (t, J = 9.0 Hz, 1H), 6.60 (d, J = 9.0 Hz, 1H), 6.47 (s, 1H), 3.44 (dd, J = 14.4, 7.2 Hz, 4H), 1.23 (t, J = 7.2 Hz, 6H). ^{13}C NMR (151 MHz, $CDCl_3$) δ 177.64, 160.38, 157.35, 152.49, 149.94, 136.94, 133.89, 130.07, 129.78, 128.60, 109.71, 108.36, 100.83, 97.26, 91.34, 89.85, 45.10, 12.43. HRMS

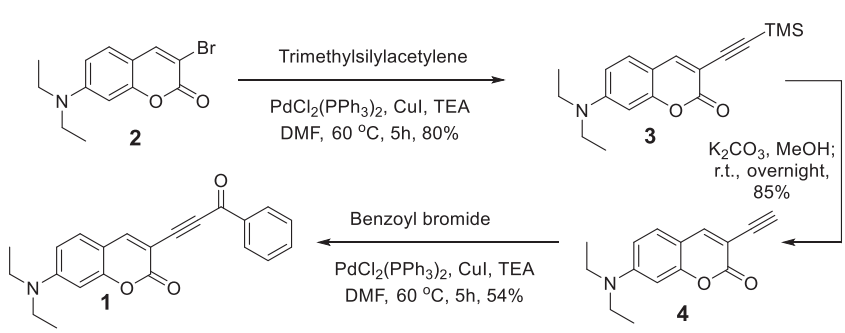

Scheme 2. Synthetic route of probe **1**.

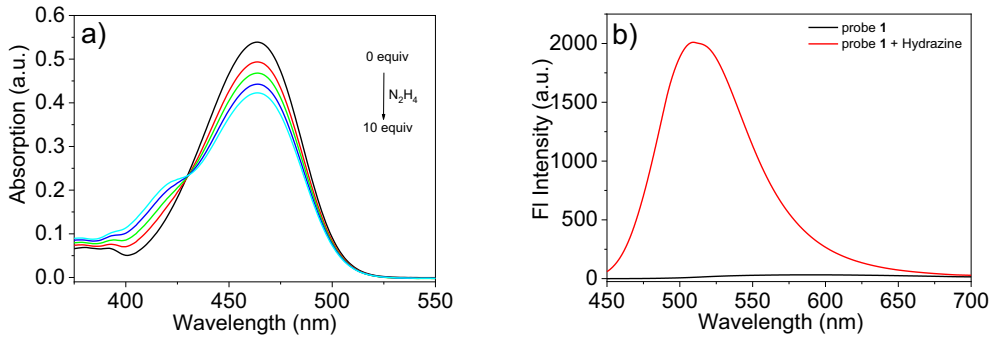

Fig. 1. (a) UV–vis spectra of probe **1** (20 μM) to hydrazine (0, 3, 5, 7, 10 Equiv) and fluorescence emission of probe **1** (20 μM) to hydrazine (10 Equiv) (b) in PBS (20 mM, pH 7.4, 30% CH_3CN).

(ESI): $[M + Na]^+$, calcd $C_{22}H_{19}NNaO_3$: m/z = 368.1263, found 368.1260.

2.3. MTT assay

HeLa cells were cultured in DMEM supplemented with 10% fetal calf serum at 37 °C in 5% CO_2. Cells were seeded in a 96-well plate. After overnight culture, cells were incubated with each concentration of probe for 12 h. To identify cell viability, 0.5 mg/mL of MTT (Sigma) media was added to cells for 4 h and the produced formazan was dissolved in 150 μL of dimethyl sulfoxide (DMSO) and read at OD 490 nm with a Spectramax microwell plate reader.

2.4. Cell imaging

The cell imaging experiments were divided into three groups. First group cells were only treated with probe **1** (10 μM) for 60 min. The next two groups' cells were pro-incubated N_2H_4 (50 μM or 150 μM) for 20 min, washed with PBS three times to remove excess hydrazine, and then incubated with probe **1** (10 μM) for 60 min. After washing as descript above, cells were used for imaging immediately. The cells were imaged with the cyan channel (475–550 nm, excitation at 405 nm).

3. Results and discussion

3.1. Design and synthesis

The coumarin scaffold has been widely applied in the design of small-molecule fluorescent chemosensors because of its high fluorescence quantum yield, strong light stability, good structural modifiability, and excellent biocompatibility [60]. Meanwhile, the PET effect is a general strategy for constructing fluorescent probes. In this work, the ynone structure was introduced into the 3-position of the 7-diethylamino-coumarin. The carbonyl group was expected to quench the fluorescence of coumarin by PET effect, and at the same time was served as the recognizing group. After reaction with hydrazine, the pyrazole ring formed could not quench the fluorescence, and the intramolecular hydrogen bonding formed could be contributing to producing a large "*turn-on*" fluorescence response (Scheme 1).

As shown in Scheme 2, the synthetic route was referred to as the reported literature [61]. Compound **2** was coupled with trimethylsilylacetylene to provide compound **3**, which was transformed into compound **4** by removing trimethylsilyl. The alkynyl group was further coupled with benzoyl bromide to provide probe **1**. The structure of all compounds was confirmed by ^{1}H NMR, ^{13}C NMR spectra and HRMS. The detailed synthesis of compounds **2** was shown in the Supporting Information.

3.2. Spectra response of probe **1** toward hydrazine

With probe **1** in hand, we first studied the UV–vis spectra and emission spectra of probe **1**. As shown in Fig. 1a, the probe solution showed the maximum absorption peak at 464 nm. With the addition of hydrazine, the intensity of the absorption peak at 464 nm decreased, and a new absorption band appeared at 415 nm appeared. The isosbestic point at 430 nm suggested the formation of a new product. In the following experiment, we chose 430 nm as the excitation wavelength. Probe **1** exhibited weak fluorescence emission (quantum yield Φ = 0.001) in PBS buffer solution (20 mM, pH 7.4, 30% CH_3CN), while after the addition of hydrazine, the obvious fluorescence enhancement at 508 nm could be observed (Φ = 0.093) (Fig. 1b).

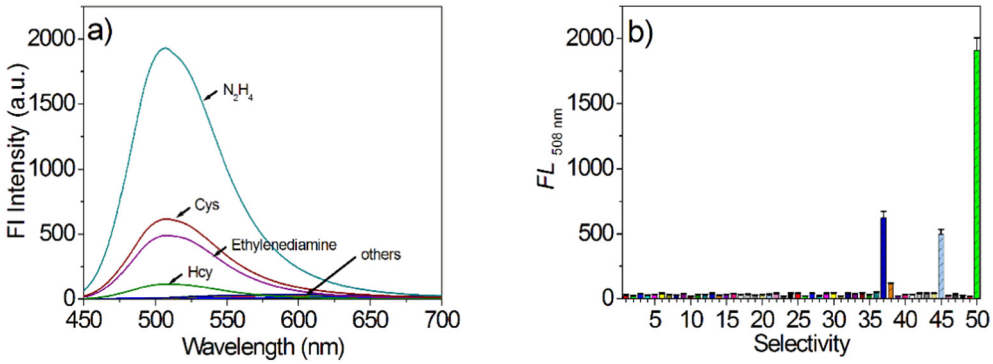

Fig. 2. Fluorescence responses of probe **1** (20 μM) to hydrazine (10 Equiv) and other species (20 Equiv). Each spectrum was recorded after 12 h of reaction in PBS (20 mM, pH 7.4, 30% CH_3CN) at room temperature. (1. Probe **1** only, 2. K^+, 3. Ag^+, 4. Ca^{2+}, 5. Cu^{2+}, 6. Mg^{2+}, 7. Zn^{2+}, 8. Pb^{2+}, 9. Ni^{2+}, 10. Cd^{2+}, 11. Mn^{2+}, 12. Hg^{2+}, 13. Fe^{2+}, 14. Fe^{3+}, 15. Al^{3+}, 16. Co^{3+}, 17. NH_4^+, 18. Cl^-, 19. Br^-, 20. I^-, 21. NO_3^-, 22. NO_2^-, 23. ClO_4^-, 24. AcO^-, 25. *t*-$BuOO^-$, 26. N_3^-, 27. HSO_3^-, 28. SO_4^{2-}, 29. CO_3^{2-}, 30. SO_3^{2-}, 31. PO_4^{3-}, 32. Vc, 33. H_2O_2, 34. HClO, 35. NO, 36. H_2S, 37. Cys, 38. Hcy, 39. GSH, 40. ammonia, 41. hydroxylamine, 42. aniline, 43. methylamine, 44. triethylamine, 45. ethylenediamine, 46. urea, 47. thiourea, 48. lysine, 49. hydrazinobenzene, 50. hydrazine).

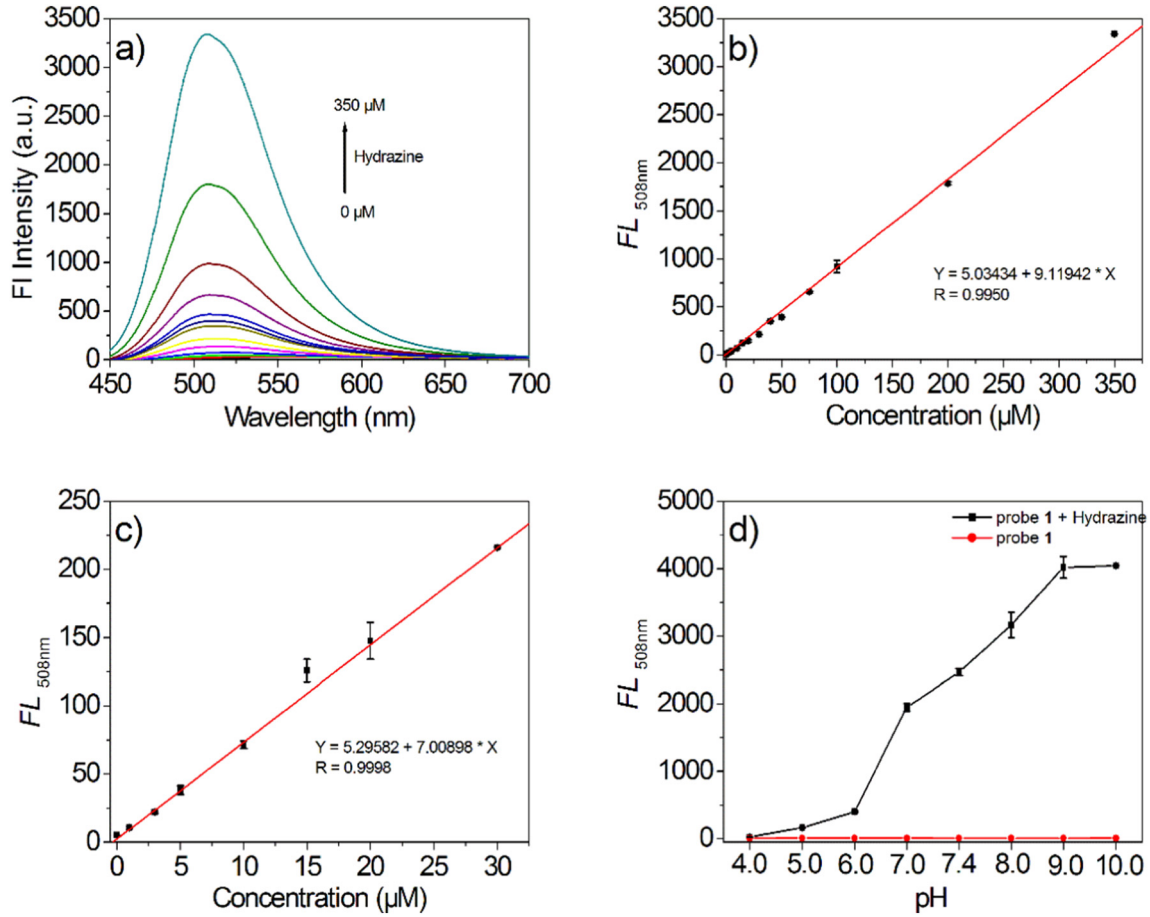

Fig. 3. (a) The titration experiments of probe **1** (20 μM) to different concentrations of hydrazine (0–350 μM). (Each spectrum was recorded after 12 h of reaction in PBS (20 mM, pH 7.4, 30% CH_3CN) at room temperature.) (b) The linear relationship between the fluorescence intensity of probe **1** at 480 nm and the concentration of hydrazine (0–350 μM). (c) The changes in the fluorescence intensity at 508 nm observed for probe **1** as a function of hydrazine concentration (0–30 μM). (d) The fluorescence intensity of probe **1** at 508 nm during different pH values in presence and absence of hydrazine (200 μM).

The selectivity is the crucial property of the fluorescent probe. We then examined the fluorescence response of probe **1** toward a range of environmental and biological interfering compounds. These related compounds conclude cations (K^+, Ag^+, Ca^{2+}, Cu^{2+}, Mg^{2+}, Zn^{2+}, Pb^{2+}, Ni^{2+}, Cd^{2+}, Mn^{2+}, Hg^{2+}, Fe^{2+}, Fe^{3+}, Al^{3+}, Co^{3+}, NH_4^+), anions (Cl^-, Br^-, I^-, NO_3^-, NO_2^-, ClO_4^-, AcO^-, *t*-$BuOO^-$, N_3^-, HSO_3^-, SO_4^{2-}, CO_3^{2-}, SO_3^{2-}, PO_4^{3-}), ascorbic acid (Vc), endogenous active species (H_2O_2, HClO, NO, H_2S, GSH, Cys, Hcy), amine compounds (ammonia, hydroxylamine, aniline, methylamine, triethylamine, ethylenediamine, urea, thiourea, lysine) and hydrazine analogues (hydrazinobenzene). As shown in Figs. 2, 20 equivalents of interfering substances could not cause obvious fluorescence changes except Cys and ethylenediamine. On the contrary, 10 equivalents of hydrazine could induce drastic emission changes. These results suggested that probe **1** can detect hydrazine with high selectivity.

We further performed the titration experiments to evaluate the sensitivity of the probe. As shown in Fig. 3a, with the increase of hydrazine concentration, the emission gradually enhanced in intensity. The fluorescence intensity increased about 600 times in the presence of 17.5 equivalent of hydrazine, and even in the presence of 0.5 equivalent hydrazine, the fluorescence intensity could be enhanced 10 times. By further data analysis, the fluorescence intensity at 508 nm is linearly dependent ($r = 0.9950$) with the concentration of hydrazine between 0 and 350 μM (Fig. 3b). The detection limit is calculated to be 267 nM (8.55 ppb) according to the $3\sigma/k$ method, which was lower than the EPA accepted the minimum threshold limit value (Fig. 3c). These results demonstrated that probe **1** is highly sensitivity to hydrazine. We also evaluated the suitable working pH range for the application of probe **1** and found a broad working pH range from 6.0 to 10.0 for the application of the probe (Fig. 3d).

3.3. Mechanism of probe *1* toward hydrazine

To further get insight into the relationship between the optical response of probe **1** to hydrazine with the structure, we carried out DFT calculations using a b3lyp/6-311d method [62]. As shown in Fig. 4, for probe **1**, the level of the lowest unoccupied molecular orbital (LUMO) of coumarin (−0.66 eV) is lower than that of ynone structure (−1.30 eV), thus coumarin served as the electron acceptor, and its fluorescence could be quenched by PET effect. After reaction with hydrazine, the level of LUMO of coumarin (−0.66 eV) is higher than that of pyrazole structure (−0.16 eV), PET effect disappeared. We also tested the HRMS spectra of the product of the probe reaction with hydrazine. A peak at $m/z = 360.1710$ ($M + H^+$) also suggested that hydrazine induced pyrazole structure formation (Scheme 1).

3.4. Fluorescence microscopy imaging

Encouraged by the above results, we then sought to examine whether probe **1** can detect hydrazine in living cells. The MTT assay was first carried out to evaluate the cytotoxicity. The results suggest that the probe **1** has no obvious toxicity to the living cells (Fig. S1). Next, HeLa cells were treated with the probe in the absence or presence of hydrazine and then fluorescence imaging. As shown in Fig. 5, the cells treated with only probe **1** showed no fluorescence, while cells pretreated with hydrazine and then incubated with probe **1** displayed

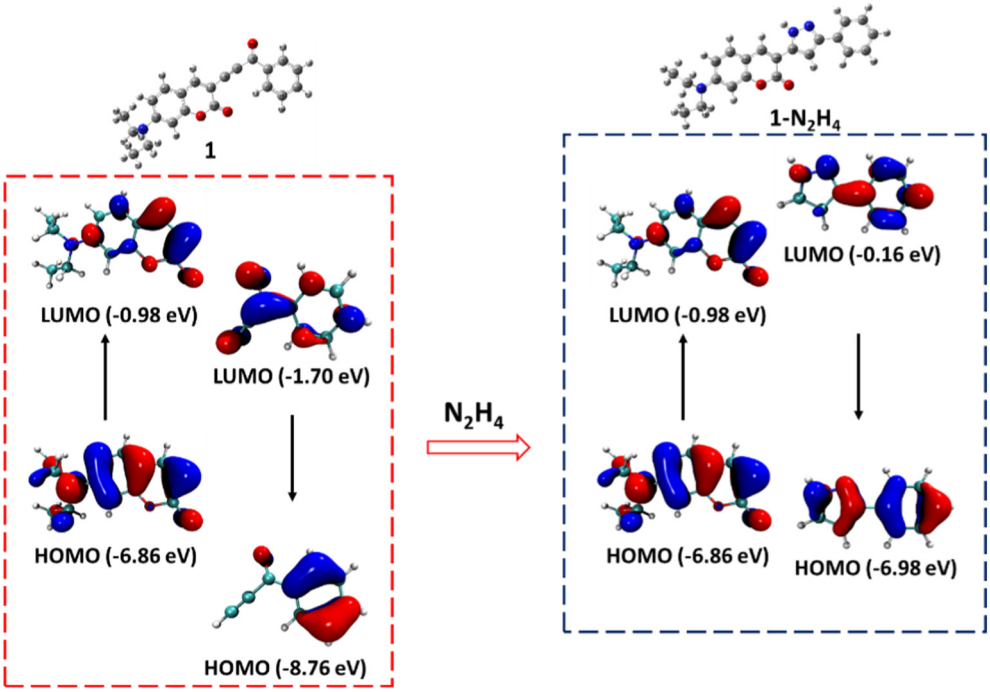

Fig. 4. HOMO-LUMO energy levels and the interfacial plots of the molecular orbitals for probe **1** and **1-N_2H_4**. The orbitals of **1** and **1-N_2H_4** are calculated at the DFT level using a b3lyp/6-311d method.

obvious green fluorescence. Moreover, the higher the concentration of hydrazine pre-treated, the stronger the fluorescence emerged (Fig. 5b and c). The above results indicated that probe **1** can be used for bioimaging hydrazine in living cells.

3.5. Hydrazine detection in real water samples

To evaluate the efficacy of probe **1** in real samples, the probe was used to monitoring hydrazine in spring water and river water. As shown in Table 1, the concentration of hydrazine detected by probe **1** showed a good match with the concentration of hydrazine added. The recovery values are moreover 90%, which implied probe **1** is capable of quantitative determination of hydrazine in real water samples.

4. Conclusions

In summary, we developed here a coumarin-fused fluorescence probe for the detection of hydrazine. The coumarin moiety with high

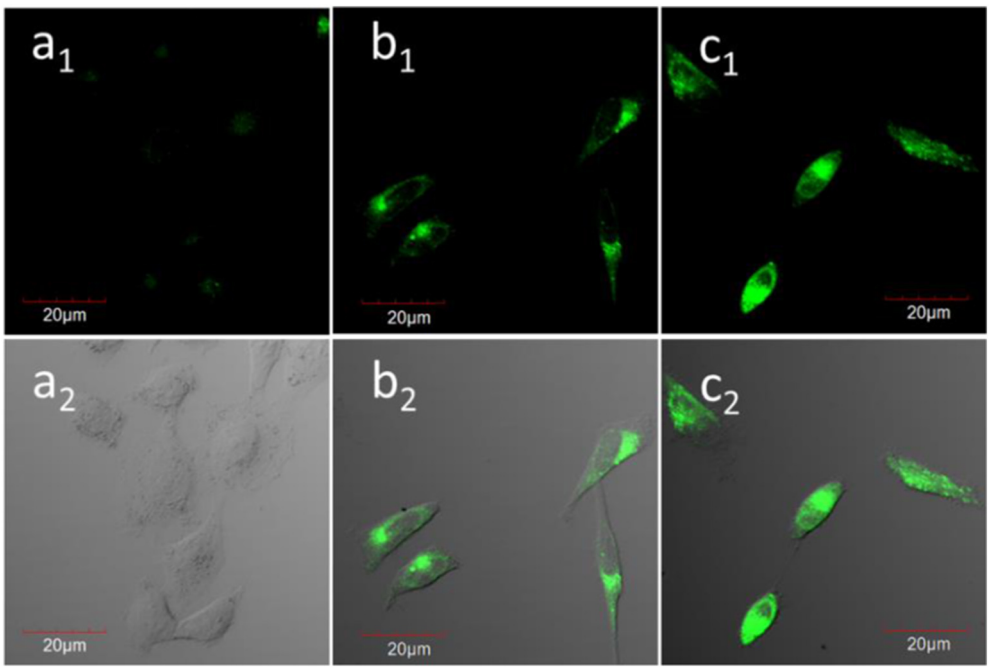

Fig. 5. Confocal fluorescence imaging of HeLa cells. Cells were only treated with probe **1** (5 μM) for 60 min (a). Cells were first treated with hydrazine (50 μM, b) or (150 μM, c) for 20 min, then washed with DMEM, and treated with probe **1** (5 μM) for 60 min. Excitation 405 nm, emission 475–550 nm, and scale bar 20 μm.

Table 1
Determination of hydrazine in spring water and river water sample.

Samples	Hydrazine (μM)		Recovery (%)
	Added	Detected	
Spring water	2.5	2.29 ± 0.12	91.6
	10	10.7 ± 0.32	107
	50	45.1 ± 2.32	90.2
River water	2.5	2.51 ± 0.08	100.4
	10	9.1 ± 0.51	91
	50	53.3 ± 1.19	106.6

fluorescence quantum yield was served as the fluorophore, and the ynone part was chosen as hydrazine reactive group. The probe showed high selectivity (fluorescence *off-on* response was approx. 600 fold) and sensitivity (the detection limit was 267 nM). The sensing mechanism was confirmed by DFT calculation and HRMS spectra. The probe can be successfully used to image hydrazine in cells and detect hydrazine in real water samples. We further expect that the probe could be applied in tissue imaging.

Declaration of competing interest

We declare that we do not have any commercial or associative interest that represents a conflict of interest in connection with the work submitted.

Acknowledgments

This work was supported by the National Natural Science Foundation of China (21605034), the Natural Science Foundation of Hebei Province (B2019201918, B2018201234), the Foundation of Hebei Education Department (QN2017015), and Science Technology Research and Development Guidance Program Project of Baoding City (18ZF315).

Appendix A. Supplementary data

Supplementary data to this article can be found online at https://doi.org/10.1016/j.saa.2020.118075.

References

[1] I. Cruz Vieira, K. Omuro Lupetti, O. Fatibello-Filho, Sweet potato (Ipomoea batatas (L.) Lam.) tissue as a biocatalyst in a paraffin/graphite biosensor for hydrazine determination in boiler feed water, Anal. Lett. (14) (2002) 2221–2231.
[2] A. Umar, M.M. Rahman, S.H. Kim, Y.-B. Hahn, Zinc oxide nanonail based chemical sensor for hydrazine detection, Chem. Commun. (2008) 166–168.
[3] H.E. Malone, Determination of mixtures of hydrazine and 1,1-dimethylhydrazine, Anal. Chem. 33 (1961) 575–577.
[4] R.B. Channon, M.B. Joseph, E. Bitziou, A.W.T. Bristow, A.D. Ray, J.V. Macpherson, Electrochemical flow injection analysis of hydrazine in an excess of an active pharmaceutical ingredient: achieving pharmaceutical detection limits electrochemically, Anal. Chem. 87 (2015) 10064–10071.
[5] F. Gao, Q. Wang, N. Gao, Y. Yang, F. Cai, M. Yamane, F. Gao, H. Tanaka, Hydroxyapatite/chemically reduced graphene oxide composite: environment-friendly synthesis and high-performance electrochemical sensing for hydrazine, Biosens. Bioelectron. 97 (2017) 238–245.
[6] A.D. Smolenkov, O.A. Shpigun, Direct liquid chromatographic determination of hydrazines: a review, Talanta 102 (2012) 93–100.
[7] J.-A. Oh, H.-S. Shin, Simple and sensitive determination of hydrazine in drinking water by ultra-high-performance liquid chromatography-tandem mass spectrometry after derivatization with naphthalene-2,3-dialdehyde, J. Chromatogr. A 1395 (2015) 73–78.
[8] J. Du, J. Lu, Hydrazine-induced post-chemiluminescence phenomenon of permanganate-luminol reaction and its applications, Luminescence 19 (2004) 328–332.
[9] K.H. Nguyen, Y. Hao, W. Chen, Y. Zhang, M. Xu, M. Yang, Y.-N. Liu, Recent progress in the development of fluorescent probes for hydrazine, Luminescence 33 (2018) 816–836.
[10] S.K. Manna, A. Gangopadhyay, K. Maiti, S. Mondal, A.K. Mahapatra, Recent developments in fluorometric and colorimetric chemodosimeters targeted towards hydrazine sensing: present success and future possibilities, Chemistryselect 4 (2019) 7219–7245.
[11] C. Hu, W. Sun, J.F. Cao, P. Gao, J.Y. Wang, J.L. Fan, F.L. Song, S.G. Sun, X.J. Peng, A ratiometric near-infrared fluorescent probe for hydrazine and its in vivo applications, Org. Lett. 15 (2013) 4022–4025.
[12] Y. Sun, D. Zhao, S.W. Fan, L. Duan, A 4-hydroxynaphthalimide-derived ratiometric fluorescent probe for hydrazine and its in vivo applications, Sensor. Actuat. B-Chem. 208 (2015) 512–517.
[13] J.J. Zhang, L.L. Ning, J.T. Liu, J.X. Wang, B.F. Yu, X.Y. Liu, X.J. Yao, Z.P. Zhang, H.X. Zhang, Naked-eye and near-infrared fluorescence probe for hydrazine and its applications in in vitro and in vivo bioimaging, Anal. Chem. 87 (2015) 9101–9107.
[14] X. Xia, F. Zeng, P. Zhang, J. Lyu, Y. Huang, S. Wu, An ICT-based ratiometric fluorescent probe for hydrazine detection and its application in living cells and in vivo, Sensor. Actuat. B-Chem. 227 (2016) 411–418.
[15] J. Ma, J. Fan, H. Li, Q. Yao, J. Xia, J. Wang, X. Peng, Probing hydrazine with a near-infrared fluorescent chemodosimeter, Dyes Pigments 138 (2017) 39–46.
[16] C.T. Liu, F. Wang, T. Xiao, B. Chi, Y.H. Wu, D.R. Zhu, X.Q. Chen, The ESIPT fluorescent probes for N_2H_4 based on benzothiazol and their applications for gas sensing and bioimaging, Sensor. Actuat. B-Chem. 256 (2018) 55–62.
[17] T. Li, J. Liu, L. Song, Z. Li, Q. Qi, W. Huang, A hemicyanine-based fluorescent probe for hydrazine detection in aqueous solution and its application in real time bioimaging of hydrazine as a metabolite in mice, J. Mater. Chem. B 7 (2019) 3197–3200.
[18] Y. Song, G. Chen, X. Han, J. You, F. Yu, A highly sensitive near-infrared ratiometric fluorescent probe for imaging of mitochondrial hydrazine in cells and in mice models, Sensor. Actuat. B-Chem. 286 (2019) 69–76.
[19] X. Jia, X. Li, X. Geng, C. Nie, P. Zhang, C. Wei, X. Li, A seminaphthorhodafluor-based near-infrared fluorescent probe for hydrazine and its bioimaging in living systems, Spectrochim. Acta A 223 (2019), 117307.
[20] M.G. Choi, J. Hwang, J.O. Moon, J. Sung, S.K. Chang, Hydrazine-selective chromogenic and fluorogenic probe based on levulinated coumarin, Org. Lett. 13 (2011) 5260–5263.
[21] S.S. Zhu, W.Y. Lin, L. Yuan, Development of a near-infrared fluorescent probe for monitoring hydrazine in serum and living cells, Anal. Methods 5 (2013) 3450–3453.
[22] S.L. Yu, S.X. Wang, H.Z. Yu, Y. Feng, S.T. Zhang, M.Z. Zhu, H. Yin, X.M. Meng, A ratiometric two-photon fluorescent probe for hydrazine and its applications, Sensor. Actuat. B-Chem. 220 (2015) 1338–1345.
[23] A.K. Mahapatra, R. Maji, K. Maiti, S.K. Manna, S. Mondal, S.S. Ali, S. Manna, P. Sahoo, S. Mandal, M.R. Uddin, D. Mandal, A BODIPY/pyrene-based chemodosimetric fluorescent chemosensor for selective sensing of hydrazine in the gas and aqueous solution state and its imaging in living cells, RSC Adv. 5 (2015) 58228–58236.
[24] Z. Ju, D. Li, D. Zhang, D. Li, C. Wu, Z. Xu, An ESIPT-based fluorescent probe for hydrazine detection in aqueous solution and its application in living cells, J. Fluoresc. 27 (2017) 679–687.
[25] S. Goswami, S. Das, K. Aich, B. Pakhira, S. Panja, S.K. Mukherjee, S. Sarkart, A chemodosimeter for the ratiometric detection of hydrazine based on return of ESIPT and its application in live-cell imaging, Org. Lett. 15 (2013) 5412–5415.
[26] Y. Qian, J. Lin, L.J. Han, L. Lin, H.L. Zhu, A resorufin-based colorimetric and fluorescent probe for live-cell monitoring of hydrazine, Biosens. Bioelectron. 58 (2014) 282–286.
[27] X.D. Jin, C.Z. Liu, X.M. Wang, H. Huang, X.Q. Zhang, H.J. Zhu, A flavone-based ESIPT fluorescent sensor for detection of N_2H_4 in aqueous solution and gas state and its imaging in living cells, Sensor. Actuat. B-Chem. 216 (2015) 141–149.
[28] Y. Hao, Y. Zhang, K. Ruan, W. Chen, B. Zhou, X. Tan, Y. Wang, L. Zhao, G. Zhang, P. Qu, M. Xu, A naphthalimide-based chemodosimetric probe for ratiometric detection of hydrazine, Sensor. Actuat. B-Chem. 244 (2017) 417–424.
[29] Z. Lu, W. Fan, X. Shi, Y. Lu, C. Fan, Two distinctly separated emission colorimetric NIR fluorescent probe for fast hydrazine detection in living cells and mice upon independent excitations, Anal. Chem. 89 (2017) 9918–9925.
[30] L. Cui, C.F. Ji, Z.X. Peng, L. Zhong, C.H. Zhou, L.L. Yan, S. Qu, S.P. Zhang, C.S. Huang, X.H. Qian, Y.F. Xu, Unique Tr-output optical probe for specific and ultrasensitive detection of hydrazine, Anal. Chem. 86 (2014) 4611–4617.
[31] L. Cui, Z.X. Peng, C.F. Ji, J.H. Huang, D.T. Huang, J. Ma, S.P. Zhang, X.H. Qian, Y.F. Xu, Hydrazine detection in the gas state and aqueous solution based on the Gabriel mechanism and its imaging in living cells, Chem. Commun. 50 (2014) 1485–1487.
[32] M.V.R. Raju, E.C. Prakash, H.C. Chang, H.C. Lin, A facile ratiometric fluorescent chemodosimeter for hydrazine based on Ing-Manske hydrazinolysis and its applications in living cells, Dyes Pigments 103 (2014) 9–20.
[33] F. Ali, A.H. A, N. Taye, D.G. Mogare, S. Chattopadhyay, A. Das, Specific receptor for hydrazine: mapping the in situ release of hydrazine in live cells and in an in vitro enzymatic assay, Chem. Commun. 52 (2016) 6166–6169.
[34] B. Li, Z. He, H. Zhou, H. Zhang, W. Li, T. Cheng, G. Liu, Reaction based colorimetric and fluorescence probes for selective detection of hydrazine, Dyes Pigments 146 (2017) 300–304.
[35] J.L. Fan, W. Sun, M.M. Hu, J.F. Cao, G.H. Cheng, H.J. Dong, K.D. Song, Y.C. Liu, S.G. Sun, X.J. Peng, An ICT-based ratiometric probe for hydrazine and its application in live cells, Chem. Commun. 48 (2012) 8117–8119.
[36] Y.Q. Tan, J.C. Yu, J.K. Gao, Y.J. Cui, Y. Yang, G.D. Qian, A new fluorescent and colorimetric probe for trace hydrazine with a wide detection range in aqueous solution, Dyes Pigments 99 (2013) 966–971.
[37] M.D. Sun, J. Guo, Q.B. Yang, N. Xiao, Y.X. Li, A new fluorescent and colorimetric sensor for hydrazine and its application in biological systems, J. Mater. Chem. B 2 (2014) 1846–1851.
[38] S.I. Reja, N. Gupta, V. Bhalla, D. Kaur, S. Arora, M. Kumar, A charge transfer based ratiometric fluorescent probe for detection of hydrazine in aqueous medium and living cells, Sensor. Actuat. B-Chem. 222 (2016) 923–929.
[39] R. Zhang, C.-J. Zhang, Z. Song, J. Liang, R.T.K. Kwok, B.Z. Tang, B. Liu, AIEgens for real-time naked-eye sensing of hydrazine in solution and on a paper substrate: structure-dependent signal output and selectivity, J. Mater. Chem. C 4 (2016) 2834–2842.

[40] Z.X. Li, W.Y. Zhang, C.X. Liu, M.M. Yu, H.Y. Zhang, L. Guo, L.H. Wei, A colorimetric and ratiometric fluorescent probe for hydrazine and its application in living cells with low dark toxicity, Sensor. Actuat. B-Chem. 241 (2017) 665–671.
[41] J.-Y. Wang, Z.-R. Liu, M. Ren, W. Lin, 2-Benzothiazoleacetonitrile based two-photon fluorescent probe for hydrazine and its bio-imaging and environmental applications, Sci. Rep. 7 (2017) 1530.
[42] X. Yang, Y. Liu, Y. Wu, X. Ren, D. Zhang, Y. Ye, A NIR ratiometric probe for hydrazine "naked eye" detection and its imaging in living cell, Sensor. Actuat. B-Chem. 253 (2017) 488–494.
[43] N. Meher, S. Panda, S. Kumar, P.K. Iyer, Aldehyde group driven aggregation-induced enhanced emission in naphthalimides and its application for ultradetection of hydrazine on multiple platforms, Chem. Sci. 9 (2018) 3978–3985.
[44] Y. Jung, I.G. Ju, Y.H. Choe, Y. Kim, S. Park, Y.-M. Hyun, M.S. Oh, D. Kim, Hydrazine exposé: the next-generation fluorescent probe, ACS Sens 4 (2019) 441–449.
[45] J. Li, Y. Cui, C. Bi, S. Feng, F. Yu, E. Yuan, S. Xu, Z. Hu, Q. Sun, D. Wei, J. Yoon, Oligo (ethylene glycol)-functionalized ratiometric fluorescent probe for the detection of hydrazine in vitro and vivo, Anal. Chem. 91 (2019) 7360–7365.
[46] J. Li, J. Liu, J.W.Y. Lam, B.Z. Tang, Poly(arylene ynonylene) with an aggregation-enhanced emission characteristic: a fluorescent sensor for both hydrazine and explosive detection, RSC Adv. 3 (2013) 8193–8196.
[47] S. Goswami, S. Das, K. Aich, D. Sarkar, T.K. Mondal, A coumarin based chemodosimetric probe for ratiometric detection of hydrazine, Tetrahedron Lett. 55 (2014) 2695–2699.
[48] B. Roy, S. Halder, A. Guha, S. Bandyopadhyay, Highly selective sub-ppm naked-eye detection of hydrazine with conjugated-1,3-diketo probes: imaging hydrazine in Drosophila larvae, Anal. Chem. 89 (2017) 10625–10636.
[49] Y. Cheng, J. Dai, C. Sun, R. Liu, T. Zhai, X. Lou, F. Xia, An intracellular H_2O_2-responsive AIEgen for the peroxidase-mediated selective imaging and inhibition of inflammatory cells, Angew. Chem. Int. Ed. 57 (2018) 3123–3127.
[50] W.-N. Wu, H. Wu, Y. Wang, X.-J. Mao, X.-L. Zhao, Z.-Q. Xu, Y.-C. Fan, Z.-H. Xu, A highly sensitive and selective off-on fluorescent chemosensor for hydrazine based on coumarin beta-diketone, Spectrochim. Acta A 188 (2018) 80–84.
[51] X. Dai, Z.-Y. Wang, Z.-F. Du, J.-Y. Miao, B.-X. Zhao, A simple but effective near-infrared ratiometric fluorescent probe for hydrazine and its application in bioimaging, Sensor. Actuat. B-Chem. 232 (2016) 369–374.
[52] T. Tang, Y.-Q. Chen, B.-S. Fu, Z.-Y. He, H. Xiao, F. Wu, J.-Q. Wang, S.-R. Wang, X. Zhou, A novel resorufin based fluorescent "turn-on" probe for the selective detection of hydrazine and application in living cells, Chin. Chem. Lett. 27 (2016) 540–544.
[53] W. Chen, W. Liu, X.J. Liu, Y.Q. Kuang, R.Q. Yu, J.H. Jiang, A novel fluorescent probe for sensitive detection and imaging of hydrazine in living cells, Talanta 162 (2017) 225–231.
[54] Y.B. Ding, S. Zhao, Q.Q. Wang, X. Yu, W.H. Zhang, Construction of a coumarin based fluorescent sensing platform for palladium and hydrazine detection, Sensor. Actuat. B-Chem. 256 (2018) 1107–1113.
[55] X. Shi, F. Huo, J. Chao, C. Yin, A ratiometric fluorescent probe for hydrazine based on novel cyclization mechanism and its application in living cells, Sensor. Actuat. B-Chem. 260 (2018) 609–616.
[56] Y. Liu, D.D. Ren, J.J. Zhang, H. Li, X.F. Yang, A fluorescent probe for hydrazine based on a newly developed 1-indanone-fused coumarin scaffold, Dyes Pigments 162 (2019) 112–119.
[57] C. Wu, H. Xu, Y. Li, R. Xie, P. Li, X. Pang, Z. Zhou, H. Li, Y. Zhang, A "naked-eye" colorimetric and ratiometric fluorescence probe for trace hydrazine, Anal. Methods 11 (2019) 2591–2596.
[58] X.R. Shi, C.X. Yin, Y.B. Zhang, Y. Wen, F.J. Huo, A novel ratiometric and colorimetric fluorescent probe for hydrazine based on ring-opening reaction and its applications, Sensor. Actuat. B-Chem. 285 (2019) 368–374.
[59] D. Purohit, C.P. Sharma, A. Raghuvanshi, A. Jain, K.S. Rawat, N.M. Gupta, J. Singh, M. Sachdev, A. Goel, First dual responsive "turn-on" and "ratiometric" AIEgen probe for selective detection of hydrazine both in solution and the vapour phase, Chem. Eur. J. 25 (2019) 4660–4664.
[60] D. Cao, Z. Liu, P. Verwilst, S. Koo, P. Jangjili, J.S. Kim, W. Lin, Coumarin-based small-molecule fluorescent chemosensors, Chem. Rev. 119 (2019) 10403–10519.
[61] K.M. Zhang, W. Dou, P.X. Li, R. Shen, J.X. Ru, W. Liu, Y.M. Cui, C.Y. Chen, W.S. Liu, D.C. Bai, A coumarin-based two-photon probe for hydrogen peroxide, Biosens. Bioelectron. 64 (2015) 542–546.
[62] M.J. Frisch, H.B. Schlegel, G.E. Scuseria, M.A. Robb, J.R. Cheeseman, Gaussian 09, Revision C.01, Gaussian, Inc., Wallingford, CT, USA, 2009.